

**Table I.** Arrhenius Activation Energies ( $E_A$ ) and Delocalizabilities ( $D_r^{(R)}$ ) for H abstractions from alkanes by  $\text{CH}_3\cdot$  and  $\text{CF}_3\cdot$  Radicals

alkane <sup>a</sup>	$E_A^-$ ( $\text{CH}_3\cdot$ ) <sup>b</sup>	$D_r^{(R)}$ ( $\text{CH}_3\cdot$ ), <sup>c</sup> $\beta$	$E_A^-$ ( $\text{CF}_3\cdot$ ) <sup>d</sup>	$D_r^{(R)}$ ( $\text{CF}_3\cdot$ ), <sup>e</sup> $\beta$
$\text{CH}_4$	60.9	$-1.10 \times 10^{-1}$	46.9	$-1.13 \times 10^{-1}$
$\text{CH}_3\text{CH}_3$	50.0	$-1.16 \times 10^{-1}$	35.2	$-1.18 \times 10^{-1}$
$\text{CH}_3\text{CH}_2\text{-}$ $\text{C}^*\text{H}_3$	48.7	$-1.17 \times 10^{-1}$		
$\text{CH}_3\text{C}^*\text{H}_2\text{-}$ $\text{CH}_3$	43.3	$-1.20 \times 10^{-1}$	26.8	$-1.26 \times 10^{-1}$
$\text{CH}_3\text{CH}_2\text{CH}_2\text{-}$ $\text{C}^*\text{H}_3$	49.1	$-1.17 \times 10^{-1}$		
$\text{CH}_3\text{CH}_2\text{C}^*\text{-}$ $\text{H}_2\text{CH}_3$	40.7	$-1.20 \times 10^{-1}$	23.9	$-1.25 \times 10^{-1}$
$(\text{CH}_3)_3\text{C}^*\text{H}$	34.4	$-1.24 \times 10^{-1}$	19.7	$-1.26 \times 10^{-1}$
$\text{C}(\text{CH}_3)_4$	50.4	$-1.17 \times 10^{-1}$	35.2	$-1.20 \times 10^{-1}$

<sup>a</sup> \* indicates the hydrogen abstracted. <sup>b</sup> For gas-phase reactions in  $\text{kJ mol}^{-1}$ .<sup>10</sup> <sup>c</sup> With  $E_{\text{SOMO}}(\text{CH}_3\cdot) = -4.23 \text{ eV}$ .<sup>2-4</sup> <sup>d</sup> Gas-phase results in  $\text{kJ mol}^{-1}$  as cited in ref 11. <sup>e</sup> With  $E_{\text{SOMO}}(\text{CF}_3\cdot) = -6.25 \text{ eV}$ .<sup>2-4</sup>

**Table II.** Hydrogen Abstractions from 1-Fluorobutane by Chlorine Atoms. Logarithm of the Relative Rate Constants ( $\ln k_{\text{rel}}$ ) and Delocalizability ( $D_r^{(R)}$ )<sup>6</sup> for Two Conformations

	$\text{C}_1$	$\text{C}_2$	$\text{C}_3$	$\text{C}_4$
$\ln k_{\text{rel}}^a$	-0.105	0.531	1.308	0
$D_r^{(R)}, \beta 180^\circ$ <sup>b,c</sup>	$-1.57 \times 10^{-1}$	$-1.41 \times 10^{-1}$	$-1.48 \times 10^{-1}$	$-1.38 \times 10^{-1}$
$D_r^{(R)}, \beta 60^\circ$ <sup>b,c</sup>	$-1.58 \times 10^{-1}$	$-1.43 \times 10^{-1}$	$-1.51 \times 10^{-1}$	$-1.40 \times 10^{-1}$

<sup>a</sup> From the relative selectivities of chlorination in the gas phase at  $78^\circ\text{C}$ .<sup>13</sup> <sup>b</sup> Values for the  $180^\circ$  and  $60^\circ$  conformations at the  $\text{C}_1\text{-C}_2$  bond. All other C-C bonds with  $180^\circ$  conformation. <sup>c</sup> With  $E_{\text{SOMO}}(\text{Cl}\cdot) = -8.34 \text{ eV}$ .<sup>2-4</sup>

linear correlation between the activation energies for H abstraction by  $\text{CH}_3\cdot$  and  $\text{CF}_3\cdot$  radicals and the delocalizabilities.

Thus the principle of maximum overlap<sup>7</sup> using MINDO/3 data<sup>2-4</sup> may serve well in predicting the relative activation energies and (in consideration of the similar  $A$  factors<sup>10,11</sup>) the relative rates of free-radical hydrogen-abstraction reactions. Obviously steric influences<sup>12</sup> can be neglected.

As shown with 1-fluorobutane as an example (Table II, Figure 2), a polar factor only seems to be important for abstraction reactions at the halogen-bearing C atom ( $\text{C}_1$ ).

**Acknowledgments.** This work was supported by grants from the Fonds der Chemischen Industrie and the Land Niedersachsen.

## References and Notes

- (1) K. Riemenschneider, Dissertation, Technische Universität Braunschweig, West Germany, 1977.
- (2) H. Bartels, Dissertation, Technische Universität Braunschweig, West Germany, 1978.
- (3) R. C. Bingham, M. J. S. Dewar, and D. H. Lo, *J. Am. Chem. Soc.*, **97**, 1294 (1975).
- (4) Quantum Chemistry Program Exchange (QCPE), program no. 308, Chemistry Department, Indiana University, Bloomington, Ind.
- (5) See, for example, D. C. Nonhebel and J. C. Walton, "Free Radical Chemistry", University Press, Cambridge, England, 1974.
- (6) It seems remarkable that the first and only approach of this kind for alkyl radical H abstraction using simple LCAO-MO data was, to our knowledge, performed 16 years ago: K. Fukui, H. Kato, and T. Yonezawa, *Bull. Chem. Soc. Jpn.*, **35**, 1475 (1962).
- (7) K. Fukui, "Theory of Orientation and Stereoselection", Springer Verlag, West Berlin and Heidelberg, 1975.
- (8)  $\alpha = E_{\text{SOMO}}$ ,  $\epsilon_i$  = energy of the  $i$ th MO of the alkane;  $c_{ri}$  = coefficient of the  $i$ th AO in the  $r$ th MO of the alkane;  $\beta$  = resonance integral.
- (9) I. Fleming, "Frontier Orbitals and Organic Chemical Reactions", Wiley, London, London-New York-Toronto, 1976.
- (10) As cited in ref 5, p 241.
- (11) S. H. Jones and E. Whittle, *Int. J. Chem. Kinet.*, **2**, 479 (1970).
- (12) For example, the back strain as discussed by C. Rüchardt, *Angew. Chem.*,

- 82**, 845; *Angew. Chem., Int. Ed. Engl.*, **9**, 830 (1970).  
(13) P. S. Fredricks and J. M. Tedder, *Chem. Ind. (London)*, 490 (1959).

H. Bartels, W. Eichel, K. Riemenschneider, P. Boldt\*  
Lehrstuhl B für Organische Chemie  
der Technischen Universität  
Braunschweig, Postfach 33 29  
D-3300 Braunschweig, West Germany  
Received June 26, 1978

## Theoretical ab Initio Calculations of Deformation Densities in Some Binuclear Metal Complexes

Sir:

The ab initio Hartree-Fock method has been applied recently to the calculation of electronic deformation density distributions<sup>1</sup> in the vicinity of transition metal atoms.<sup>3,4</sup> We report here the first theoretical calculations of deformation densities for binuclear metal complexes immediately comparable with experimental works. Deformation density maps were obtained for  $t\text{-}[(\pi\text{-C}_5\text{H}_5)\text{Fe}(\text{CO})_2]_2$  (I) and  $(\eta^5\text{-C}_5\text{H}_5\text{Ni})_2\text{-CH}\equiv\text{CH}$  (II). The molecular density is issued from ab initio calculations<sup>5</sup> at the SCF level with double- $\zeta$  basis sets for the valence shells. The atomic density distributions were calculated for each atom with the same basis set as that used in the molecular calculation. The atoms were taken to be neutral and in their ground states. The contours are based upon a grid having an increment of 0.2 au. Positive and negative contours were drawn with an interval of  $0.03 \text{ e}(\text{au})^{-3}$  from 0 to  $\pm 0.18 \text{ e}(\text{au})^{-3}$ .

**Bis(dicarbonyl- $\pi$ -cyclopentadienyliron) (I).** Figure 1 shows the deformation density distribution for I in the plane containing the iron atoms and the terminal carbonyls. A comparison with an experimental deformation density map drawn for the same plane<sup>8</sup> shows that all significant features of the experimental map are correctly reproduced,<sup>19</sup> especially the four density peaks around each metal separated by a negative zone colinear to the Fe-CO bond. The lack of significant features in the region located around the Fe-Fe line, noticed about the experimental deformation density map,<sup>8</sup> is also confirmed. The absence of residues in the metal-metal direction seems to be consistent with the fact that our molecular SCF wave function does not display any significant direct metal-metal bond. This conclusion is based upon the small negative value of the Mulliken overlap population between iron atoms<sup>10</sup> and upon an analysis of the valence shell molecular orbitals, especially of the HOMO which exhibits a strong back-bonding character from the  $d_{yz}$  orbital of iron toward the bridging carbonyls.<sup>12</sup> This analysis illustrates the concept of delocalized multicentered linkages of bridging carbonyl ligands to two or three metals proposed by Chini<sup>13</sup> and Braterman<sup>14</sup> and already corroborated by SCF calculations on  $\text{Co}_2(\text{CO})_8$ <sup>15</sup> and  $\text{Fe}_3(\text{CO})_{12}$ .<sup>11</sup>

**$\pi$ -Acetylenebis(cyclopentadienylnickel) (II).** This complex is supposed to present a direct metal-metal bond because of electron counting and of the very short metal-metal distance ( $2.345 \text{ \AA}$ ).<sup>7</sup> However, the nature of this bond "straight" or "bent" away from the acetylene<sup>18</sup> is still controversial. The "bent" metal-metal bond model was found by Teo and co-workers to correspond to the character of the HOMO in several  $\text{Fe}_2(\text{CO})_6\text{X}_2$ -type dimers.<sup>16</sup> However, experimental density deformation maps obtained by Wang and Coppens for II exhibit density accumulation with two maxima along the Ni-Ni line, thus favoring the "straight" bond model.<sup>7</sup> We depict in Figure 2 the electron density contour map obtained for the

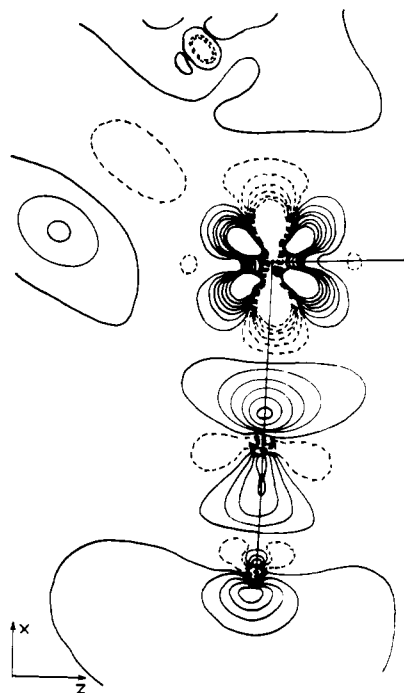


**Figure 1.** Section of the deformation density distribution of complex I by a plane containing the terminal carbonyl and the Fe-Fe line. Contour interval:  $0.03 \text{ e}(\text{au})^{-3}$ . Deformation densities beyond  $\pm 0.18 \text{ e}(\text{au})^{-3}$  are not represented. Dashed contours are for negative and solid lines for zero and positive deformation densities.

HOMO of II, in the plane containing the two Ni atoms and perpendicular to the acetylene C-C bond. It clearly indicates the bent nature of the Ni-Ni bond obtained from our wave function. In Figure 3, showing the deformation density map obtained for the same region of space, the region of the bent metal-metal bond corresponds to a zone of electron deficiency with a double minimum at  $0.34 \text{ \AA}$  from the metal. Beyond this point, the deficiency decreases and finally vanishes at the midpoint of the Ni-Ni line. This scheme seems in contradiction with the notion of electron pairing, which intuitively implies an accumulation of electron density between the bonded atoms. However, the lack of density accumulation at the center of the bond could be explained by the weak overlap between metal atoms<sup>8</sup> and the large regions of electron deficiency colinear to the  $d_{z^2}$  orbitals involved in the Ni-Ni bond can be related to the high population ( $1.6 \text{ e}$ ) of each spherically averaged d-orbital in the ground-state configuration of nickel,  $3d^8 4s^2$ .<sup>20</sup>

Contrary to the case of complex I, the comparison of the computed density distribution with experimental results leads to a serious disagreement, especially in the regions of the metal atoms. The four nonoverlapping regions of electron accumulation around each metal displayed in Figure 3 are consistent with the feature most currently observed in octahedral-like transition metal complexes, namely a concentration in directions corresponding to the threefold axes of the octahedron.<sup>8,17,21,22</sup> The experimental map obtained by Wang and Coppens<sup>7</sup> for the same plane does not show any significant electron-deficient region, but only two zones of charge accumulation around each metal, one oriented toward the center of the  $\text{C}_5\text{H}_5$  ring and the other toward the ethylene C-C bond. These features were interpreted in terms of a trigonal rather than octahedral symmetry around the nickel atom.<sup>7</sup>

Deformation density around the acetylene ligand is displayed in Figures 3 and 4. Both maps show a displacement of the density maximum away from the C-C line in a direction away from the nickel atoms. This is an important point of agreement with experiment,<sup>7</sup> but differences at the qualitative level are still found in this region. The peaks displayed on the

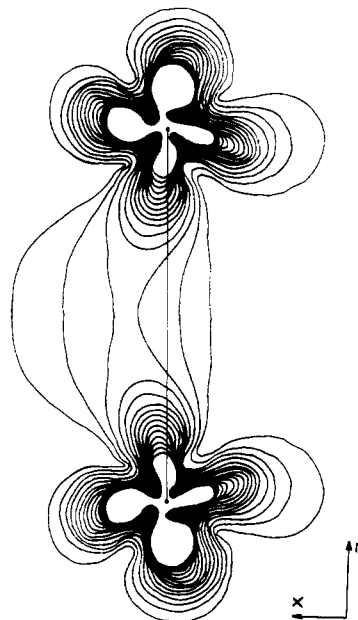


**Figure 2.** Electron density contour map for the HOMO of complex II in the plane containing two nickel atoms and the midpoint of the acetylene C-C bond. Contour interval:  $0.01 \text{ e}(\text{au})^{-3}$ .

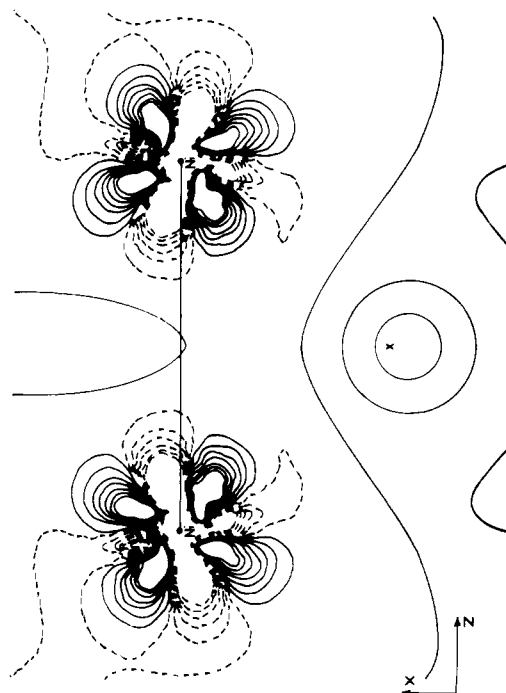


**Figure 3.** Section of the deformation density distribution of complex II in the plane containing two nickel atoms and the midpoint of the acetylene C-C bond. Contours as in Figure 1.

C-H bonds (Figure 4), which are not observed experimentally, can be attributed to the neglect of the thermal motion of the hydrogens.<sup>23</sup> However, the presence of a unique peak above the C-C line and the location of the electron-deficient regions around the carbon atoms, though characteristic of a carbon-carbon bond, are less easy to reconcile with the experimental features.

It is not excluded that configuration interaction would induce a modification of d-orbital populations leading to a qualitative change in computed deformation density maps in the vicinity of the metal atoms.<sup>3</sup> However, the fair agreement with experimental deformation density obtained for complex I may give some confidence about the reliability of the

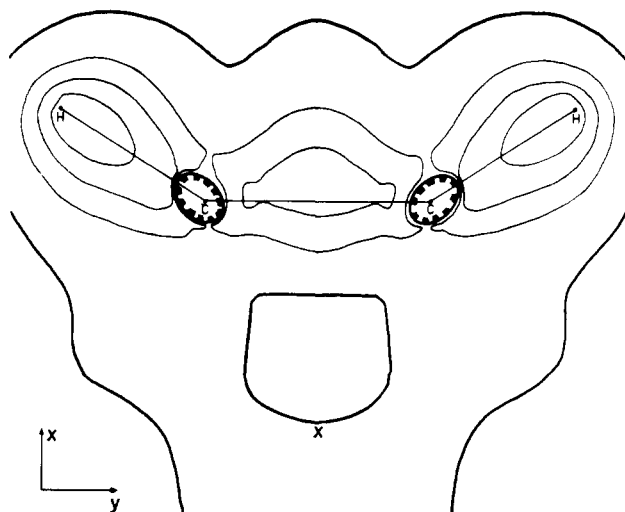


Figure 4. Section of the deformation density of complex II in the plane containing the acetylene ligand and the midpoint of the Ni-Ni line. Contour interval:  $0.03 \text{ e}(\text{au})^{-3}$ . Negative deformation densities beyond  $-0.09 \text{ e}(\text{au})^{-3}$  are not represented. Bold line is for zero deformation density.

map similarly computed for II. In order to obtain more possibilities of comparison with experimental work, calculations were started on other binuclear complexes, including  $\text{Cr}_2(\text{O}_2\text{CH})_4$ .

**Acknowledgments.** Calculations have been carried out at the Centre de Calcul du C.N.R.S. in Strasbourg-Cronembourg. We thank the staff for their cooperation. We are also very grateful to Dr. B. Rees for useful discussions and collaboration throughout this work.

## References and Notes

- (1) The electronic deformation density distribution,  $\Delta\rho(r)$ , is defined as the difference between a molecular electronic density distribution and the superposition of spherically averaged atomic distributions.<sup>2</sup>
- (2) D. R. Salahub, A. E. Foti, and V. H. Smith, Jr., *J. Am. Chem. Soc.*, **99**, 8067 (1977), and references therein.
- (3) H. Johansen, *Acta Crystallogr., Sect. A*, **32**, 353 (1976).
- (4) I. Shim, Ph.D. Thesis, Lyngby, Denmark, 1977.
- (5) The LCAO-MO-SCF calculations were carried out with the Asterix system of programs<sup>6</sup> using gaussian basis sets 11, 7, 5 for Ni and Fe, 8, 4 for first-row atoms, and 4 for hydrogen contracted to basis sets minimal for the inner shells and the  $(n+1)s$  and  $(n+1)p$  shells of Ni and Fe, but split for the valence shells. Geometries used correspond to the most recent experimental determinations.<sup>7,8</sup>
- (6) M. Bénard, A. Dedieu, J. Demuyneck, M.-M. Rohmer, A. Strich, and A. Veillard, Asterix: a system of programs for the Univac 1110, unpublished work. M. Bénard, *J. Chim. Phys.*, **73**, 413 (1976).
- (7) Y. Wang and P. Coppens, *Inorg. Chem.*, **15**, 1122 (1976).
- (8) A. Mitschler, B. Rees, and M. S. Lehmann, *J. Am. Chem. Soc.*, **100**, 3390 (1978).
- (9)  $1 \text{ e}(\text{au})^{-3} = 6.74876 \text{ e} \text{ \AA}^{-3}$ .
- (10) The Fe-Fe overlap population is  $-0.05$ . This value has to be compared for instance to a similarly computed overlap population of  $+0.16$  between the nonbridged iron atoms in  $\text{Fe}_3(\text{CO})_{12}$ .<sup>11</sup>
- (11) M. Bénard, unpublished work.
- (12) The z axis is supposed collinear to the Fe-Fe direction.
- (13) P. Chini, *Inorg. Chim. Acta, Rev.*, **2**, 31 (1968).
- (14) P. S. Braterman, *Struct. Bonding (Berlin)*, **10**, 57 (1971).
- (15) See note 19 in ref 16.
- (16) B. K. Theo, M. B. Hall, R. F. Fenske, and L. F. Dahl, *Inorg. Chem.*, **14**, 3103 (1975).
- (17) B. Rees and A. Mitschler, *J. Am. Chem. Soc.*, **98**, 7918 (1976).
- (18) D. L. Thorn and R. Hoffmann, *Inorg. Chem.*, **17**, 126 (1978).
- (19) A quantitative comparison should allow for thermal motion and limited resolution which reduce the sharpest features in the experimental map.<sup>17</sup> As a matter of fact, both electron accumulation and deficiencies are found larger by the calculation than by the experiment, as already noticed by Johansen for other metal complexes.<sup>3</sup>
- (20) The Mulliken population analysis of the molecular wave function attributes a population of 1.77 to 1.94 e to each d orbital, except  $d_{z^2}$ . As expected from the presence of a  $\sigma$  bond, the population of  $d_{z^2}$  is significantly lower, 1.48 e, that is, less than the atomic averaged orbital population.
- (21) B. Rees and P. Coppens, *Acta Crystallogr., Sect. B*, **29**, 2516 (1973); M. Iwata and Y. Saito, *ibid.*, **29**, 822 (1973); F. Marumo, M. Isobe, Y. Saito, T. Yagi, and S. Akimoto, *ibid.*, **30**, 1904 (1974).
- (22) If complexes I and II are considered as octahedral, one of the threefold axes

becomes collinear to the direction metal center of the  $\text{C}_5\text{H}_5$  ring.  
(23) E. D. Stevens, J. Rys, and P. Coppens, *J. Am. Chem. Soc.*, **100**, 2324 (1978).

M. Bénard

Laboratoire de Chimie Quantique  
Institut Le Bel, Université Louis Pasteur  
4 rue B. Pascal, 67000 Strasbourg, France

Received June 14, 1978

## On the Hartree-Fock Theory of Local Regions in Molecules

Sir:

The direct determination of localized orbitals for large molecules has received increasing attention in the past years.<sup>1</sup> This concept is useful in particular if different local basis sets are used for the expansion of localized orbitals belonging to different localization centres (subsystems). Several authors have discussed the use of such local or fluctuating basis sets. Matsuoka<sup>2</sup> and the present authors<sup>3</sup> have modified the Adams-Gilbert equations<sup>1</sup> for this case; Mehler<sup>4</sup> has derived a variational method for nonorthogonal group functions based on local energy functionals; Payne<sup>5</sup> has given equations for the determination of the Hartree-Fock determinant with the lowest energy under the variational restriction imposed by the local basis sets. It is the last paper by Payne on which we want to comment.

We start from a set of (occupied) localized orbitals  $\{\varphi_{i\alpha}\}$  and a corresponding set of local basis functions  $\{\chi_{ip}\}$ ;  $i$  denotes the subsystem,  $\alpha$  refers to different orbitals, and  $p$  refers to different basis functions belonging to the same subsystem. We expand each orbital in terms of basis functions of the same subsystem

$$|\varphi_{i\alpha}\rangle = \sum_p C_{ip,i\alpha} |\chi_{ip}\rangle \quad (1)$$

where all  $C_{ip,j\alpha}$  values with  $i \neq j$  are constrained to be zero. The reciprocal orbitals are defined by

$$|\tilde{\varphi}_{i\alpha}\rangle = \sum_{j\beta} |\varphi_{j\beta}\rangle S^{-1}_{j\beta,i\alpha} \quad (2)$$

with  $S_{j\beta,i\alpha} = \langle \varphi_{j\beta} | \varphi_{i\alpha} \rangle$ .

The energy  $E$  of the Slater determinant built up from the nonorthogonal orbitals of eq 1 depends on the nonzero orbital coefficients  $C_{ip,i\alpha}$ . The determinant with the lowest  $E$  is, of course, characterized by vanishing partial derivatives of  $E$  with respect to the  $C_{ip,i\alpha}$ :

Table I. Comparison of Results for  $\text{CH}_4$  Using (a) Payne's Equations (eq 4) and (b) a Steepest-Descent Method<sup>a</sup>

Definition of Subsystems		
subsystem	orbital	basis functions
1	1s (C)	C: $s_1$
2...5	$\sigma$ (CH)	C: $sp_1, sp_2$ H: $s_1, s_2$
Orbital Coefficients ( $\sigma_{CH}$ )		
(a) 0.41410, 0.46094, 0.21333, 0.07166		
(b) 0.38516, 0.58661, 0.19381, $-0.02778$		
Total Energy		
(a) $-39.8242$		
(b) $-39.8354$		

<sup>a</sup> A modified 4-31G basis set<sup>6</sup> is used, where the 2s and 2p groups are replaced by Gaussian lobes with distance  $0.437/\sqrt{\eta}$  from the C nucleus in the bond directions. All values are given in atomic units.